Progress In Electromagnetics Research C, Vol. 107, 173–182, 2021

Wideband CPW-Fed Oval-Shaped Monopole Antenna for Wi-Fi 5 and Wi-Fi 6 Applications

Jayshri Kulkarni[1, *] and Chow-Yen-Desmond Sim[2]

Abstract—A wideband coplanar waveguide (CPW) fed monopole antenna designed for Wi-Fi 5 and Wi-Fi 6 applications is proposed. The proposed antenna (main radiator) has a designed footprint of only $20 \times 8.7 \times 0.4\,\text{mm}^3$, which is composed of an oval-shaped ring radiator with three concentric rings and a double-T structure loaded with a J-shaped slot. The main novelty of this work is that the measured wideband operation of 34.5% (5.15–7.29 GHz) is contributed by only a single resonance at 6.2 GHz, conforming to the bandwidth requirement of Wi-Fi 5 (5.15–5.85 GHz) and Wi-Fi 6 (5.925–7.125 GHz). Furthermore, the proposed antenna also exhibits good radiation characteristics, including a gain around 2.25 dBi, a radiation efficiency above 80%, a total efficiency above 70%, and omnidirectional radiation patterns with a low magnitude of cross polarization throughout the bands of interest.

1. INTRODUCTION

Presently, there is a great demand for higher data rates due to the increasing demand in places such as multi-family housing, offices, airports, entertainment venues, and other high-density environments. Not only is there a need to improve the data rate, but it is also vital to improve the capability of a network when several devices are connected to it simultaneously. With a view to the above, a new next-generation Wi-Fi (Wireless Fidelity) standard known as Wi-Fi 6 (802.11 ax) has been developed in this journey of continuous innovation. Wi-Fi 6 is becoming very popular because it is capable of providing a maximum data rate of up to 9.6 Gb/s while maintaining strong connections even when more and more devices are added. Wi-Fi 6 standards also improve the reliability, efficiency, flexibility, security, and scalability of the network, thus allowing greater network performances. Therefore, antennas that maintain compatibility with existing standard IEEE 802.11ac (also known as Wi-Fi 5) along with conforming to the bandwidth requirement of Wi-Fi 6 simultaneously are of greater demand for next generation wireless communications.

Several antenna design techniques that exhibit multiband or wideband operations have been reported in the literature [1–16] for wireless applications. Amid these designs, dielectric resonator antennas (DRAs) are very popular as they offer high dielectric strength and no inherent conductor loss, which results in better radiation efficiency. An example of such a design has been investigated in [1], in which a DRA antenna with dimensions of $14 \times 30 \times 8\,\text{mm}^3$ has been designed for multiband operation in the WiMAX (3.4–3.69 GHz), 5G (3.3–3.6 GHz), and WLAN (5.72–5.80 GHz) bands. In [2], even though the Artificial Magnetic Conductor (AMC) applied can increase the gain of the antenna, as well as achieving multiband operations in (2.13–2.87 GHz), (3.22–4.75 GHz) and (5.54–5.86 GHz) bands, and the planar size of the antenna has a larger area of $37.26 \times 37.26\,\text{mm}^2$. To maintain a compact size antenna for multiband operations, the design method known as Complimentary Split Ring (CSR) is widely used in antenna design. In [3], CSR has been applied to achieve multiband

Received 9 November 2020, Accepted 1 December 2020, Scheduled 8 December 2020
* Corresponding author: Jayshri Kulkarni (jayah2113@gmail.com).
[1] Department of Electronics and Telecommunication Engineering, Vishwakarma Institute of Information Technology, Pune, India. [2] Department of Electrical Engineering, Feng Chia University, Taiwan.

operations across the (842–947 MHz), (2.3–2.46 GHz), and (4.98–5.16 GHz) bands. To further achieve small sizes with omnidirectional patterns, a half-wave dipole fed by microstrip balun that has dimensions of $50 \times 10 \times 1\,\text{mm}^3$ operating in the WiFi bands of (2.24–2.7 GHz) and (4.73–5.6 GHz) has been studies in [4]. To realize a flexible antenna for UMTS (1.9 GHz) and WiMAX (5.8 GHz) applications, Reference [5] has reported a flexible paper based printed antenna having dimensions of $35 \times 30\,\text{mm}^2$. To achieve very small dimensions of $17.5 \times 8\,\text{mm}^2$, Reference [6] has presented a simple multifrequency monopole antenna operating in 2.4 GHz, 3.3 GHz, and 5.8 GHz bands. Notably, the antenna designs reported in [1–6] do not cover the complete Wi-Fi 5 bands. Even though the patch antenna design in [7] has a size of $34.6 \times 33.05 \times 1.57\,\text{mm}^3$ and can cover the entire Wi-Fi 5 band, the design has used an expensive Roger substrate to fabricate the antenna. Thus, in [8–11], several unique antenna designs with very wide bandwidth for specific industry applications are introduced using a low-cost FR-4 substrate. In [8], a multiband shark-fin shorted monopole antenna (of dimensions $57 \times 40 \times 1.6\,\text{mm}^3$) for automotive applications has been investigated. Even though it can cover the (0.81–5.84 GHz) band, the reflection coefficients measured are across the −6 dB threshold, which is not a standard practice as far as wireless devices are concerned. To improve the reflection coefficient from 6 dB to 10 dB, as well as to cover multiband operations at wireless standards 3.3/5.0/5.8/6.6/9.9/15.9 GHz, the antenna structure ($44 \times 39 \times 1.6\,\text{mm}^3$) in [9] has used the split ring resonator type. However, its hexa-band characteristics can only be achieved by loading a PIN diode located at a reclined L-shaped slot in the ground plane, where the use of the diode can further increase the manufacturing complexity of the designs. To reduce the manufacturing complexity, [10, 11] present a simple monopole antenna operating in the 2.4/5 GHz WLAN bands with dimensions of $44 \times 33\,\text{mm}^2$ and $42 \times 30\,\text{mm}^2$, respectively. As wireless devices such as smartphones, laptops, notebooks, and tablets play a very crucial role for the end-user in day to day life, several antennas designed for laptop/portable devices are reported in [12–16]. Unfortunately, all the antennas reported above are unable to cover the frequency band of Wi-Fi 6.

Through the investigation of the aforementioned existing state of the arts, it is obvious that the need to design an antenna, with Wi-Fi 6 and Wi-Fi 5 operating bands simultaneously, is essential for future wireless devices. Therefore, this paper presents a novel, compact, low cost, simple structure, and easy to manufacture CPW-fed wideband printed oval-shaped monopole antenna for Wi-Fi 5 and Wi-Fi 6 applications. The proposed antenna is built on a low-cost FR-4 substrate, and the main radiator is composed of an oval-shaped ring radiator with three concentric rings and a double T-shaped structure loaded with a J-slot. The complete structure is fed using the CPW technique, and a single resonance is excited at around 6.2 GHz, which covers the 10 dB impedance bandwidth of (5.15–5.85 GHz) of Wi-Fi 5 and (5.925–7.125 GHz) of Wi-Fi 6 bands. Moreover, to validate the suitability of the proposed antenna for 802.11ax technology, simulated experimentation of an 8×8 Multi User-Multiple Input Multiple Output (MU-MIMO) antenna array has also been carried out. It is found that the array exhibits the same impedance bandwidth as presented by a single proposed antenna along with an isolation of larger than 15 dB throughout the bands of interest.

2. DESIGN AND ANALYSIS OF PROPOSED ANTENNA

Figure 1 depicts the structural layout of the proposed CPW-fed antenna with detailed dimensions. The proposed antenna is printed on a 0.4 mm thick rectangular FR-4 substrate of size $20 \times 8.7\,\text{mm}^2$ with a dielectric constant (ε_r) of 4.3 and a loss tangent ($\tan\delta$) of 0.025. The simulation is carried out using Computer Simulation Technology Microwave Studio (CST MWS) software. As mentioned earlier, the main radiator is an oval-shaped ring structure that has three concentric rings (inner radius of 0.5 mm and outer radius of 1 mm) loaded along the left, right, and top sections. The minor axis and major axis lengths of the oval-shaped ring are 6.2 mm and 12.4 mm, respectively, sharing a common width of 0.8 mm. A double-T structure is loaded and connected to the inner circumference of the oval-shaped ring structure, and it is composed of two vertical structures (the top vertical one has a size of 5 mm × 2 mm, and the bottom vertical one has a size of 3.5 mm × 2 mm) each supporting a horizontal structure (the top horizontal one has a size of 5.3 mm × 1 mm, and the bottom horizontal one has a size of 6 mm × 1 mm). Notably, a narrow horizontal slot of size (5.3 mm × 0.4 mm) is loaded to the top horizontal structure, while a bending narrow slot is loaded across the two vertical structures and the bottom horizontal structure, thereby forming the J-slot, as shown in Figure 1.

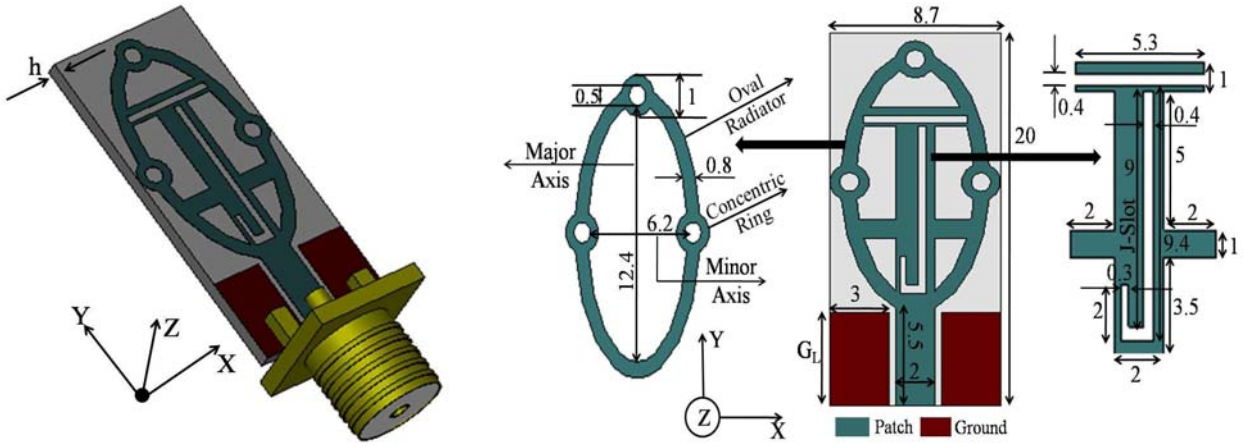

Figure 1. Detailed structural layout with dimensions of proposed antenna (All dimensions are in mm).

To give a better insight into the proposed antenna, the stepwise design is illustrated in Figure 2 and explained as follows. Initially, to induce a resonance at around 6.2 GHz, an oval-shaped ring structure radiator is designed on a 0.4 mm thick FR-4 substrate and fed using the CPW-fed technique, in which the feeding line and the two symmetrical ground planes of the CPW are of sizes $5.5 \times 2\,\text{mm}^2$ and $5 \times 3\,\text{mm}^2$, respectively. Here, major axis of the oval-shaped ring radiator is considered to be quarter-wavelength long at the resonating frequency 6.2 GHz, and it is calculated by using Equations (1) and (2) [17], whereas the minor axis length of the oval-shaped ring radiator is half the length of the major axis one.

$$\epsilon_{eff} = \frac{\epsilon_r + 1}{2} + \frac{\epsilon_r - 1}{2}\left(\frac{1}{\sqrt{1 + 12\dfrac{h}{W}}}\right) \tag{1}$$

$$L = \frac{c}{4f_r\sqrt{\epsilon_{eff}}} \tag{2}$$

In the above equations, L denotes the length of the major axis, h the height of the FR-4 substrate, W the width of the oval shaped radiator, ϵ_{eff} the effective permittivity, c the speed of light (3×10^8 m/s), and f_r the resonating frequency at 6.2 GHz. The design steps (denoted as Step-1 to Step-4) layout is illustrated in Figure 2(a), and its corresponding reflection coefficient magnitude ($|S_{11}|$) dB characteristics are depicted in Figure 2(b). From Figure 2(b), it is seen that the deployment of Step-1 (a simple oval-shaped ring radiator) can induce a resonance at around 6 GHz, but it has a narrow 10 dB impedance bandwidth of (5.6–6.2 GHz), thus unable to cover the entire Wi-Fi 5 and Wi-Fi 6 bands. To further improve the impedance matching (bandwidth) of this excited resonance, Step-2 is improvised, in which a double-T structure is loaded within the inner circumference of the oval-shaped ring structure, without disturbing the compactness of the proposed antenna. From its corresponding $|S_{11}|$ curve, a well improved 10 dB impedance bandwidth of (5.20–6.40 GHz) is seen to be achieved. However, such improvement in matching by Step-2 is still inadequate to cover the two bands of interest. Therefore, to further enhance the operating bandwidth, Step-3 is introduced, in which the J-slot is embedded into the double-T structure. Notably, this embedded J-slot in Step-3 has aided in increasing the impedance bandwidth of the antenna to (5.00–6.80 GHz), as depicted in Figure 2(b), but the bandwidth requirement of Wi-Fi 6 (5.925–7.125 GHz) remains unsatisfied. Hence, via further studies from the simulation, it is realized that the loading of three concentric rings along the left, right, and top sections of the oval-shaped ring radiator (now denoted as Step-4 or proposed antenna) can excite a very wide 10 dB impedance bandwidth of (5.08–7.23 GHz), and it can very well cover the two bands of interest ranging from 5.15 GHz to 7.125 GHz.

To further comprehend the design principle of the proposed wideband antenna, its corresponding surface current distribution (A/m) at the resonance frequency of 6.2 GHz is plotted in Figure 3(a). Here, it is visualized that an equal amount of current is flowing along the oval-shaped ring radiator, J-slot

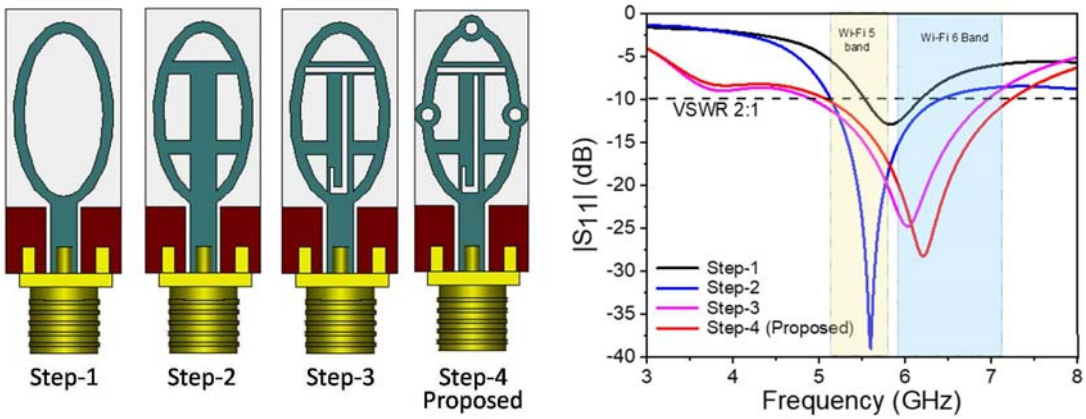

Figure 2. (a) Design steps of the proposed antenna. (b) Step-wise simulated reflection co-efficient $|S_{11}|$ (dB) of the proposed antenna.

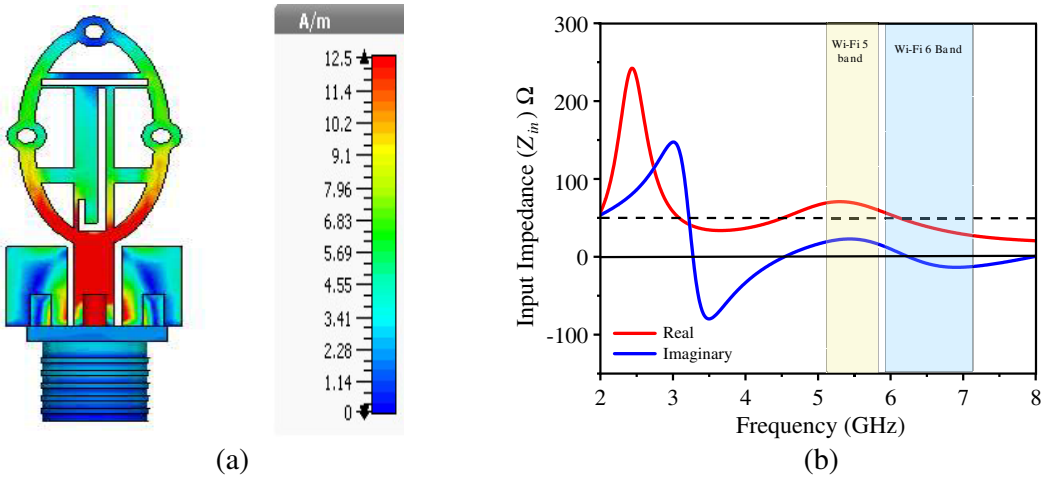

Figure 3. (a) Surface current distribution (A/m) of the proposed antenna. (b) Input impedance (Ω) versus frequency (GHz) curve of the proposed antenna.

as well as the three concentric rings, forming a near half-wavelength distribution. In order to validate the impedance matching characteristics, Figure 3(b) depicts the input impedance (Ω) versus frequency (GHz) curve of the proposed antenna. In this figure, it is clearly seen that at the resonance frequency of 6.2 GHz, the real part of the impedance is approximately equal to 50 Ω, whereas the imaginary part is approximately equal to 0 Ω. Furthermore, across the two bands of interest, the variations of the real and imaginary impedances are very slow (moderate) as well, which confirms that the proposed antenna has achieved a good impedance matching and satisfies the requirement of maximum power transfer theorem.

3. PARAMETRIC ANALYSIS OF THE PROPOSED ANTENNA

Owing to the compact size, the mirroring performance of the proposed antenna is sensitive to the variation of geometrical parameters. To illustrate the influence of essential parameters on the performance of antenna across the desired Wi-Fi 5 (5.15–5.85 GHz) and Wi-Fi 6 (5.925–7.125 GHz) bands, a vital parametric analysis has been carried out. Here, the parameters selected are height 'h' of the substrate and length 'G_L' of the symmetric ground plane, and the studies are performed by keeping all other parameters unchanged.

3.1. Influence of Substrate Height 'h' on the Performance of the Proposed Antenna

To examine the influence of substrate height 'h' on the performance of the proposed antenna, 'h' is varied from 0.2 mm to 0.8 mm in step increments of 0.2 mm, as illustrated in Figure 4. In this figure, it is observed that 'h' mainly affects the resonance and bandwidth of the proposed antenna. By increasing 'h' from 0.2 mm to 0.8 mm, the resonance (initially at 6.5 GHz) will shift linearly towards the lower frequency spectrum near 5.6 GHz, while the operating bandwidth is reduced by approximately half. Therefore, 'h' of 0.4 mm is chosen as the optimized value as it fulfills the desired bandwidth requirement as well as maintaining a low profile for the proposed antenna.

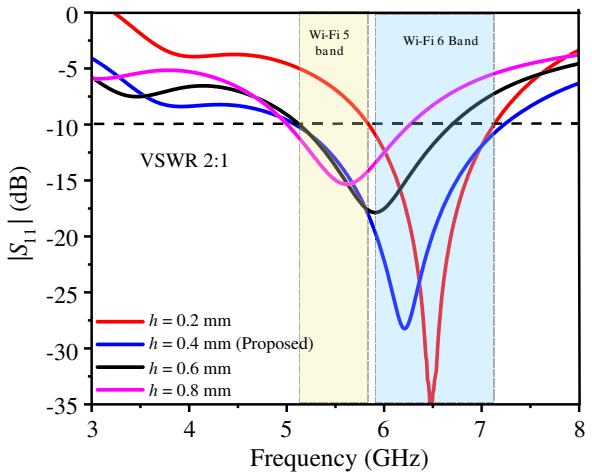

Figure 4. Influence of substrate height 'h' on the performance of the proposed antenna.

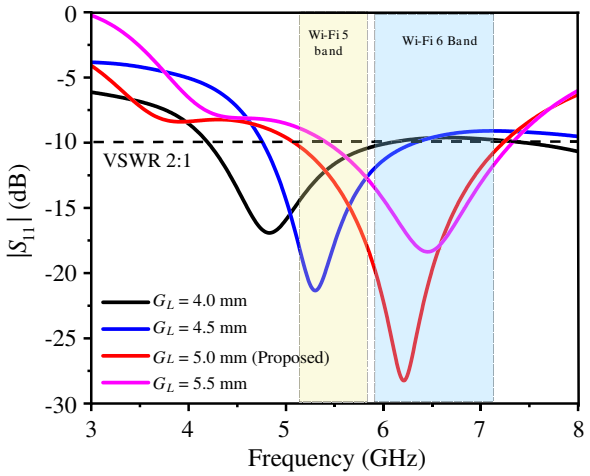

Figure 5. Influence of ground plane length 'G_L' on the impedance bandwidth of the proposed antenna.

3.2. Influence of Symmetric Ground Plane Length 'G_L' on the Performance of the Proposed Antenna

Figure 5 illustrates the influence of ground plane length 'G_L' on the impedance bandwidth of the proposed antenna. The parametric study of this parameter is very essential as it plays a very important role for impedance matching purpose. As depicted in Figure 5, as 'G_L' increases from 4 mm to 5.5 mm in step increments of 0.5 mm, the resonance shifts linearly from lower frequency (approximately 4.8 GHz) to higher frequency (approximately 6.5 GHz) spectrum. Here, 'G_L' of 5 mm is chosen as the optimized value because the desired impedance bandwidth with resonance at 6.2 GHz is obtained.

4. VALIDATION, RESULTS AND DISCUSSION OF THE PROPOSED ANTENNA

In order to validate the simulated design of the proposed antenna (based on dimensions catalogued in Figure 1), the proposed antenna was fabricated, as shown in Figure 6, and its scattering characteristics were validated by using the ROHDE & SCHWARZ ZVH8 (100 kHz–8 GHz) Vector Network Analyzer (VNA). As for its radiating characteristics such as radiation patterns, gain, and radiation efficiency, they were measured using an anechoic chamber of size $8 \times 4 \times 4\,\text{m}^3$.

4.1. Reflection Coefficient Magnitude ($|S_{11}|$) dB characteristic of Proposed Antenna

Figure 7 shows the simulated and measured $|S_{11}|$ of the proposed antenna. A good agreement between the two results is observed across the Wi-Fi 5 and Wi-Fi 6 bands. Even though there is a slight deviation between the simulated and measured $|S_{11}|$ results, it may be due to fabrication tolerances, soldering, or inaccuracies in dimensions while fabricating the proposed antenna.

Figure 6. Fabricated prototype of the proposed antenna with SMA-Type-1 connector.

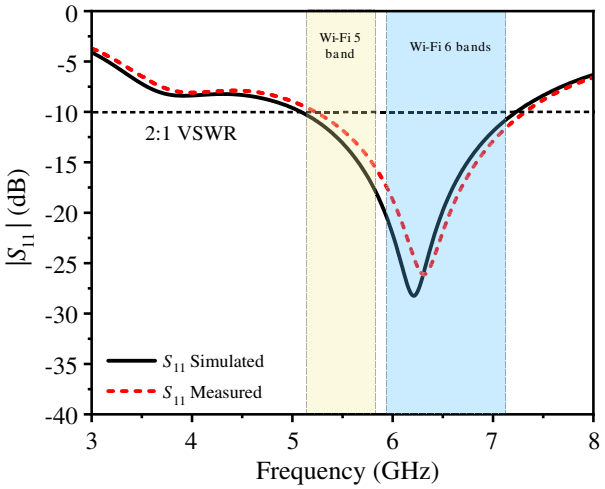

Figure 7. Measured and simulated reflection coefficient $|S_{11}|$ (dB) of the proposed antenna.

Notably, from Figure 7, it is confirmed that both simulated and measured $|S_{11}|$ curves cover the desired operating bandwidths (simulated 5.08–7.23 GHz and measured 5.15–7.29 GHz) requirement of Wi-Fi 5 and Wi-Fi 6 bands with $|S_{11}| < -25$ dB near 6.2 GHz (resonance). Therefore, the proposed antenna has achieved excellent impedance matching throughout the bands of interest.

4.2. Radiation Patterns of the Proposed Antenna

The simulated and measured two-dimensional (2D) polar radiation patterns of the proposed antenna plotted across the E-plane (x-y plane) and H-plane (y-z plane) at the resonance frequency of 6.2 GHz are shown in Figure 8. In this figure, the proposed antenna has exhibited good conventional monopole radiation patterns, in which the co-polar pattern is an omnidirectional pattern, and its corresponding cross-polar pattern is a bi-directional pattern (8-shaped). Figure 9 depicts its corresponding simulated three-dimensional (3D) radiation patterns at 6.2 GHz. It is observed that the 3D patterns are correlated with the 2D patterns with negligible side lobes. This validates that the proposed antenna exhibits very good omnidirectional radiation patterns that ensure the good strength of received and transmitted signals for wireless applications.

4.3. Gain and Efficiency of the Proposed Antenna

The simulated and measured gains and radiation efficiencies of the proposed antenna across the two bands of interest are shown in Figure 10(a). In this figure, it is observed that the simulated values are slightly higher than the measured ones, which could be due to fabrication tolerances, soldering, or slight

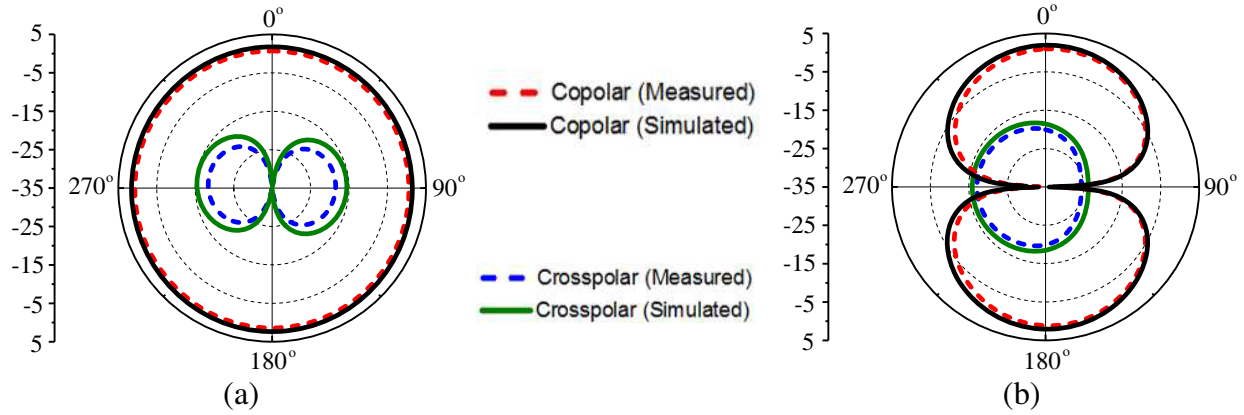

Figure 8. Simulated and measured 2D polar pattern of the proposed antenna at 6.2 GHz (a) *E*-plane and (b) *H*-plane.

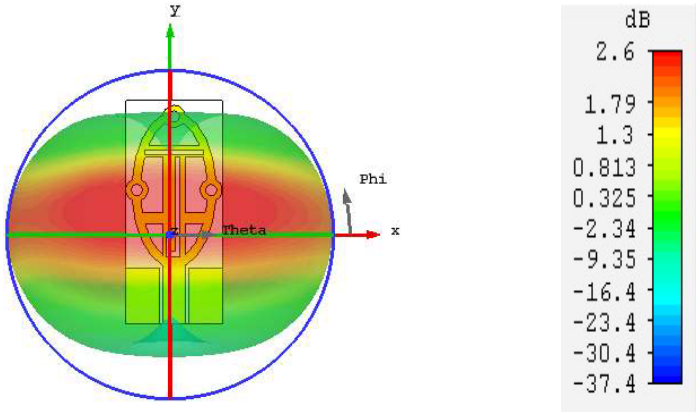

Figure 9. Simulated 3D radiation pattern of the proposed antenna at 6.2 GHz.

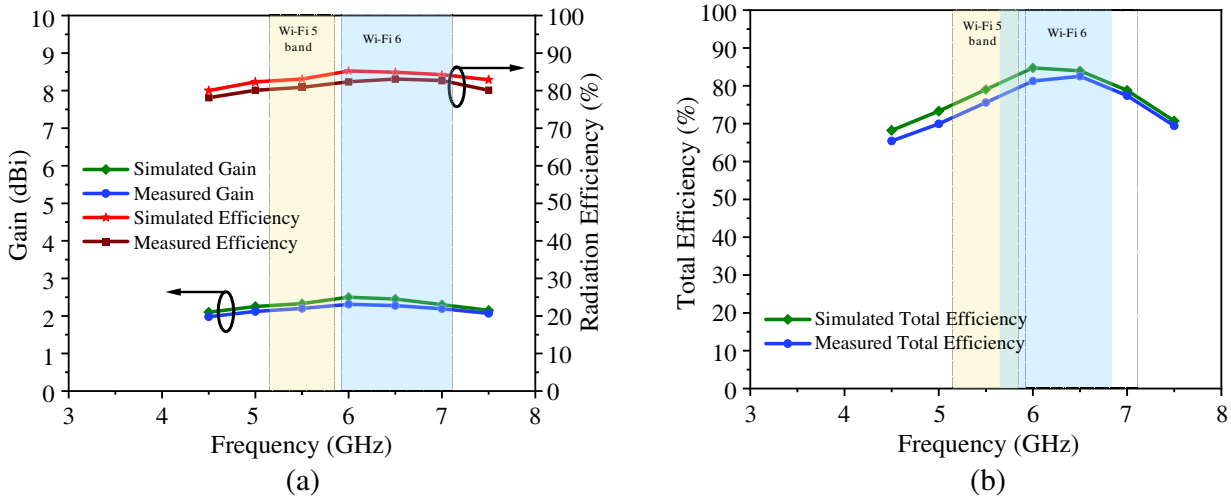

Figure 10. (a) Simulated and measured gain and radiation efficiency. (b) Simulated and measured total efficiency.

inaccuracies in dimensions while fabricating the proposed antenna. Nevertheless, Figure 10(a) affirms that the proposed antenna emanates a constant measured gain of approximately 2.25 dBi and excellent radiation efficiency greater than 80% throughout the bands of interest.

The simulated and measured total efficiencies of the proposed antenna are computed using the below formula (3) and shown in Figure 10(b).

$$\text{Total Efficiency} = \text{Radiation Efficiency} \times \left(1 - |S_{11}|^2\right) \tag{3}$$

In Equation (3), the values of $|S_{11}|$ and radiation efficiency are obtained from Figures 7 and 10(a). From Figure 10(b) it is observed that the total efficiency is well above 70% throughout the operating band. The above results ensure that the proposed antenna has good signal reception quality, which is essential for wireless operations to achieve better performance of wireless communication systems.

5. SIMULATED ANALYSIS OF THE PROPOSED MU MIMO ANTENNA

In order to validate the suitability of the proposed antenna for MU MIMO IEEE 802.11ax standard, an array of 8×8 antenna elements with a size of $83.6 \times 45\,\text{mm}^2$ is simulated using CST MWS simulator, as shown in Figure 11(a).

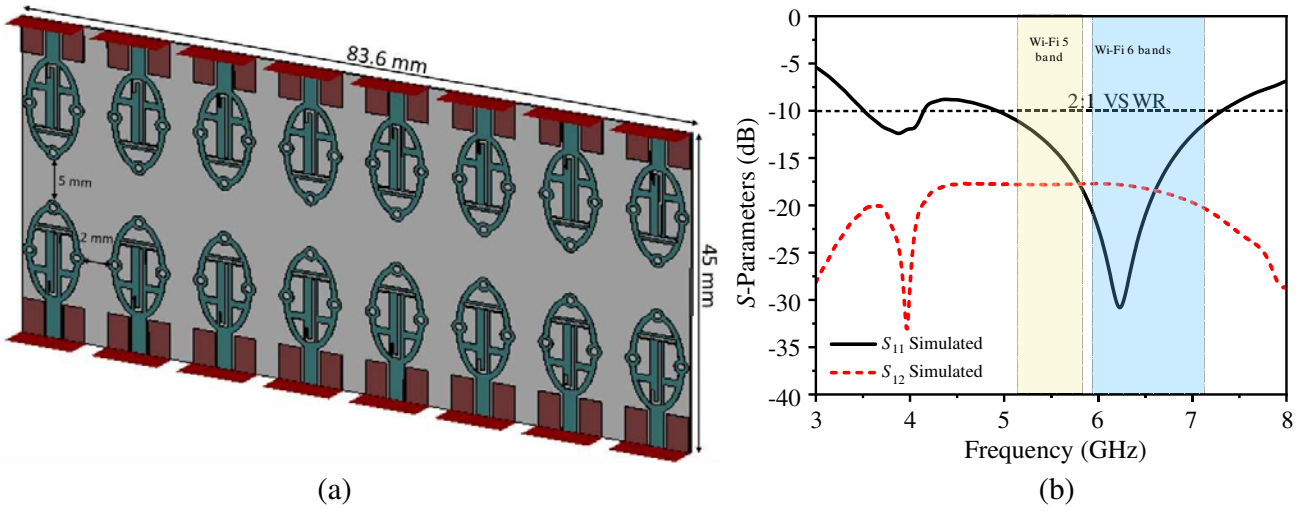

Figure 11. (a) 8×8 antenna array. (b) Simulated $|S_{11}|$ and $|S_{12}|$ of the proposed antenna array.

Here, the antenna elements are deployed horizontally with an edge to edge distance of 2 mm, whereas the vertical distance is maintained at approximately 3 mm. This deployment of 8×8 antenna elements offers better isolation of larger than 20 dB without impacting the impedance matching and impedance bandwidth at 6.2 GHz. For brevity, only $|S_{11}|$ (dB) and isolation $|S_{12}|$ (dB) curves are shown in Figure 11(b). In this figure, it is ascertained that the simulated 8×8 MIMO antenna array exhibits the same bandwidth of 2.15 GHz (5.08–7.23 GHz) as offered by the proposed antenna. Therefore, because of better performance and compact size of $83.6 \times 45\,\text{mm}^2$, the MU-MIMO antenna is a potentially good candidate for IEEE 802.11ax standards applications.

6. PERFORMANCE COMPARISON OF THE PROPOSED ANTENNA

To validate the potency of the proposed antenna, the performances (antenna size, operating bands, type of substrate used, gain, radiation efficiency, and feeding technique) of the proposed antenna are compared with the recently published pioneering state of the arts, and they are shown in Table 1. It is noteworthy that the proposed antenna has some obvious advantages over these reported ones, such as small size, cost effectiveness, and better radiation performances.

Table 1. Performance comparison of proposed antenna with recent pioneering state of arts.

Ref.	Dimension (mm^3)	Operating Bands (GHz)	Substrate	Gain (dBi)	Efficiency (%)	Feeding Technique
[1]	$14 \times 30 \times 8$	3.3/5.2/5.8	RT Duroid and Foam	4.0	80	CPW
[2]	$37.26 \times 37.26 \times 1.6$	2.4/3.3/5.8	FR-4	4.93	NG	CPW
[3]	$18 \times 22 \times 1.6$	0.9/2.4/5.2	FR-4	NG	NG	Microstrip
[4]	$50 \times 10 \times 1$	2.4/5.2	FR-4	2.09	NG	Microstrip
[5]	$35 \times 30 \times 0.12$	1.9/5.8	Flexible paper	0.512	55	CPW
[6]	$17.5 \times 8 \times 0.8$	2.4/3.3/5.8	FR-4	1.5	80	Microstrip
[7]	$34.6 \times 33.05 \times 1.57$	5	RT Duroid	7	95	Co-axial
[8]	$57 \times 40 \times 1.6$	0.8/1.7/2.4/5	FR-4	6.7	NG	Co-axial
[9]	$44 \times 39 \times 1.6$	3.3/5/6.6/9.9	FR-4	1.98	78	Microstrip
[10]	$43 \times 33 \times 1.6$	2.4/3.8/5	FR-4	5.6	NG	Microstrip
[11]	$42 \times 30 \times 1.6$	2.4/5	FR-4	4	90	Microstrip
[Proposed]	$20 \times 8.7 \times 0.4$	5/6	FR-4	2.25	80	CPW

NG: Not Given

Based on this performance comparison, some of the salient and important features of the proposed antenna are as follows:

1. The proposed antenna is compact and has smaller dimensions than [1–5, 7–11].
2. Unlike [1, 7], the proposed antenna does not require an expensive substrate.
3. The proposed antenna is very thin and can be used in next-generation wireless devices (with slim characteristics) as it has less thickness (low in profile) than [1–4, 6–11].
4. The proposed antenna has higher gain and efficiency than [4–6, 9].
5. It does not require any 3-dimensional structure [1], additional ground plane [8], or reactive component [9] for the excitation of required bands.
6. The proposed antenna is cost-effective as it does not use expensive RT-Duroid substrate unlike [1, 7], additional ground plane unlike [8], reactive components [9], and also has less fabrication cost due to its compact size unlike [1–5, 7–11].

7. CONCLUSION

The design of a novel, cost effective, and wideband printed CPW-fed oval-shaped ring monopole antenna has been successfully studied. The proposed antenna is easy to fabricate and has a compact size of $20 \times 8.7 \times 0.4\,mm^3$. Based on the excitation of only a single resonance at 6.2 GHz, a wide impedance bandwidth of 34.5% (5.15–7.29 GHz) was measured, and it can cover the desired Wi-Fi 5 (5.15–5.85 GHz) and Wi-Fi 6 (5.925–7.125 GHz) bands. Besides demonstrating good monopole radiation patterns (omnidirectional), the proposed antenna also demonstrates a constant gain of approximately 2.25 dBi, radiation efficiency of above 80%, and total efficiency of above 70% throughout the operating band. It is worth mentioning that the proposed antenna is also suitable to be used as an element of 8×8 MU-MIMO antenna for IEEE 802.11ax technologies. Therefore, owing to the simple structure, cost effectiveness, space efficiency, and good performances across the Wi-Fi 5 and Wi-Fi 6 bands, the proposed antenna is a good candidate to support the 802.11ac and 802.11ax standards for wireless applications in next-generation wireless devices.

REFERENCES

1. Guo, Q., J. Zhang, J. Zhu, and D. Yan, "A compact multiband dielectric resonator antenna for wireless communications," *Microw. Opt. Technol. Lett.*, Vol. 62, 2945–2952, 2020.
2. Gong, Y., S. Yang, B. Li, Y. Chen, F. Tong, and C. Yu, "Multi-band and high gain antenna using AMC ground characterized with four zero-phases of reflection coefficient," *IEEE Access*, Vol. 8, 171457–171468, 2020.
3. Rajalakshmi, P. and N. Gunavathi, "Compact modified hexagonal spiral resonator-based tri-band patch antenna with octagonal slot for Wi-Fi/WLAN applications," *Progress In Electromagnetics Research C*, Vol. 106, 77–87, 2020.
4. Yang, Y.-B., F.-S. Zhang, Y.-Q. Zhang, and X.-P. Li, "Design and analysis of a novel miniaturized dual-band omnidirectional antenna for WiFi applications," *Progress In Electromagnetics Research M*, Vol. 94, 95–103, 2020.
5. Aziz, A., A. Motagaly, A. Ibrahim, W. Rouby, and M. Abdalla, "A printed expanded graphite paper based dual band antenna for conformal wireless applications," *Int. J. Electron. Comm. (AEU)*, Vol. 110, 1–7, 2019.
6. Kulkarni, J. and C. Y. D. Sim, "Low-profile, compact multi-band monopole antenna for futuristic wireless applications," *2020 IEEE International Conference on Electronics, Computing and Communication Technologies (CONECCT)*, 1–5, Bangalore, India, 2020.
7. Kumar, A., A. A. Althuwayb, and M. J. Al-Hasan, "Wideband triple resonance patch antenna for 5G Wi-Fi spectrum," *Progress In Electromagnetics Research Letters*, Vol. 93, 89–97, 2020.
8. Abbasi, N., R. Langley, and S. Bashir, "Multiband shorted monopole antenna," *Journal of Electromagnetic Waves and Applications*, Vol. 28, No. 5, 618–633, 2014.
9. Saraswat, R. and M. Kumar, "A vertex-fed hexa-band frequency reconfigurable antenna for wireless applications," *Int. J. RF Microw. Comput. Aided Eng.*, Vol. 29, 1–13, 2019.
10. Jing, J., J. Pang, H. Lin, Z. Qui, and C.-J. Liu, "A multiband compact low-profile planar antenna based on multiple resonator stubs," *Progress In Electromagnetics Research Letters*, Vol. 94, 1–7, 2020.
11. Kumar, Y., R. Gangwar, and B. Kanaujia, "Asymmetrical mirror imaged monopole antenna with modified ground structure for DBDP radiations," *International Journal of Electronics*, Vol. 107, 1–24, 2020.
12. Kulkarni, J., N. Kulkarni, and A. Desai, "Development of H-shaped monopole antenna for IEEE 802.11a and HIPERLAN 2 applications in the laptop computer," *Int. J. RF Microw. Comput. Aided Eng.*, Vol. 30, No. 7, 1–14, 2020.
13. Sim, C. Y. D., C. C. Chen, X. Y. Zhang, and Y. L. Lee, "Very small-size uniplanar printed monopole antenna for dual-band WLAN laptop computer applications," *IEEE Trans. Antennas Propag.*, Vol. 65, 2916–2922, 2017.
14. Kulkarni, J., "Multi-band printed monopole antenna conforming bandwidth requirement of GSM/WLAN/WiMAX standards," *Progress In Electromagnetics Research Letters*, Vol. 91, 59–66, 2020.
15. Kulkarni, J., "An ultra-thin, dual band, sub 6 GHz, 5G and WLAN antenna for next generation laptop computers," *Circuit World*, Vol. 45, 363–370, 2020.
16. Sim, C., H. Liu, and C. Huang, "Wideband MIMO antenna array design for future mobile devices operating in the 5G NR frequency bands n77/n78/n79 and LTE band 46," *IEEE Antennas and Wireless Propagation Letters*, Vol. 19, 74–78, 2020.
17. Kulkarni, J., A. Desai, and C. Y. D. Sim, "Wideband four-port MIMO antenna array with high isolation for future wireless systems," *Int. J. Electron. Comm. (AEU)*, 2020, doi: https://doi.org/10.1016/j.aeue.2020.153507.